Construction and Building Materials 308 (2021) 125091

Contents lists available at ScienceDirect

Construction and Building Materials

journal homepage: www.elsevier.com/locate/conbuildmat

Pycnometry for assessing porosity of fine recycled aggregates

Rafael dos Santos Macedo [a,*], Carina Ulsen [a], Ana Y. Jacomo [a], Paula O. Figueiredo [a], Guilherme P. Nery [a], Daniel Uliana [a], Anette Müller [b]

[a] Universidade de São Paulo, Escola Politécnica, Department of Mining and Petroleum Engineering, Technological Characterization Laboratory, Brazil
[b] Weimar Institute of Applied Construction Research, Germany

ARTICLE INFO

Keywords:
Envelope density
Skeletal density
Porosity
Construction and demolition wastes
Fine recycled aggregates

ABSTRACT

The study extended the applications of powder pycnometry (PP) replacing the commercial enveloper for alternative envelopers (ceramic and carbon microspheres) to determine the envelope density of fine recycled aggregates (FRA) sand fraction. The properties of enveloper material such as particle size distribution, skeletal density and shape (aspect ratio and sphericity) affect the envelope density determination consequently impacts in porosity results by the association of PP and Helium pycnometry (HePyc). The porosity determination by association of HePyc and PP are comparable with mercury intrusion porosimetry analysis for medium sand fraction (0.300–1.180 mm).

1. Introduction

Construction and demolition wastes (CDW) consists of inorganic and organic materials, as concrete, masonry, excavated soil, glass, gypsum, metal, wood, plastics and others [1–3]. Concrete is the most widely applied material in construction activities, and consequently, it is also abundant in CDW in many countries [4,5]. The quality of recycled aggregates (RA) depends essentially on the composition of the precursor waste and the processing steps applied on recycling [6,7]. Therefore, some doubt about the quality and properties of recycled aggregates materials concerns the consumer market [8].

The production of coarse recycled aggregates (greater than 4.8 mm) generates about 50% of the total weight in particles below 4.8 mm (fine fraction). The fine fraction obtained after comminution process, generally is disregarded or poorly employed as components in road pavement bases [7,9]. The use of fine recycled aggregates (FRA) in construction is increasingly encouraged by governments; in general, the application of these materials is currently restricted to non-structural concrete and pavement bases in Brazil [10]. The limited application is related to the low quality of the concrete produced with FRA in comparison to the concrete produced from natural aggregates (NA) [11]. The open pores present in the cement paste are the main responsible for the "active porosity"[1] that's recycled concrete aggregates which impacts its quality and applications [12,13]. The open porosity of FRA can be correlated to the water absorption capacity, aspects such as slow kinetic water transfer of small pores and the presence of gases trapped in the pores affect the direct comparison between the properties mainly for FRA [12,14]. The measurements of water absorption in aggregates (natural or manufactured) are regulated by National and International standards and also extended to recycled aggregates [15,16]. For FRA, the water absorption is performed according to ASTM C128 standard, also known as the Cone method, the reliability of the method depends on some factors as particles shape, but the main factor responsible for the imprecision of the method is related to the operator's experience [17]. Due to imprecise factors such as fine particle loss, particles roughness [18], operator experience requirements and low repeatability, alternative methods have been studied for a more accurate procedure to assess porosity in recycled aggregates [12].

Mercury intrusion porosimetry (MIP) is one of the most applied techniques to evaluates pores size distribution, porosity and specific surface area for hydrated cementitious materials [19–22]; this technique provides information of pores between micrometers to nanometers [22,23]. Although it is a very useful characterization technique, there are four important limitations of this technique that must be considered:

- The first limitation is related to the Laplace equation, sometimes known as "Washburn equation", that considers the diameter of finite cylindrical pores for calculations, Eq.1 [23]. However, the pores of the cement paste are heterogeneous [19].

* Corresponding author at: Department of Mining and Petroleum Engineering, Polytechnic School, University of Sao Paulo, Av. Prof. Mello Moraes, 2373, Butantã, CEP 05508-030 São Paulo, SP, Brazil.

[1] Active porosity- Open pores that effectively reacts with water in the curing cement process impacting the water/cement ratio.

https://doi.org/10.1016/j.conbuildmat.2021.125091
Received 28 April 2021; Received in revised form 1 September 2021; Accepted 27 September 2021
Available online 2 October 2021

$$P_c = \frac{2\gamma\cos\theta}{r} \quad (1)$$

P_c -capillary pressure; γ- mercury surface tension; θ- mercury contact angle, usually, 130-140°; r- pore radius.

- The contact angle has a direct influence on the calculated pore size; some aspects must be considered to perform good measurements, as mercury impurities, sample surface roughness and materials composition [23]. The recycled concrete aggregates are materials characterized by high surface roughness [24], therefore it is difficult to determine the mercury contact angle.
- The mercury intrusion pressure related to the Laplace equation only establishes the pore throat diameter without considering the shape of the pores, that is established as the relationship between the throat diameter and length of the pores [19,23].
- The use of mercury requires standards practices ensuring the operator and environmental occupational safety.

The innovative methods for porosity determination involve indirect methods, such as modification in water absorption measurements for recycled aggregates by the saturated surface-dry theory (SSD) [25,26], as well as direct methods as powder pycnometry (PP) [27] and image analysis [28].

The applications of PP described in literature involve hydroxyapatite, iron ore, compressed wood pellets and granulated ribbons for envelope density evaluation. The Geopyc equipment can measure also TAP density (transverse axial pressure) applied in granulation studies for cement paste, concrete and petroleum coke samples [29–36].

The pores are also known as "voids" are not actually empty, it is filled by liquids and gases molecules. The porosity can be evaluated as interparticle and intraparticle pores, related to one particle/fragment or set of particles (Fig. 1.

To determinate agglomerate[2] volume including the interparticles and intraparticle pores are recommended to perform "TAP" and "bulk" volume analysis. The envelope volume is obtained considering only the intraparticles porosity, includes sample skeletal volume plus open pores volumes. The "skeletal" or sometimes called "apparent" volume incorporate the sample true volume plus closed pores volume. True volume is the volume of the particles excluding all types of pores [27,37].

The PP is a technique still little explored for envelope density determination, especially for fine materials. The determination of envelope density by this technique consists by involving a solid sample by a solid (quasi-fluid) enveloper that creates a solid film around each sample particles. During the measurement, a plunger vibrates pushed by an automatic external force to accommodate the enveloper on the sample surface [32]; the difference between the displacement of the plunger with and without the sample is converted to volume.

There are four main factors (Fig. 2 that affect envelope density measurements by PP. Some aspects related to the sample and enveloper materials conformance must be considered for good measurement results, such as samples/envelopers particles fragmentation, surface roughness and density [29–31].

The instrumental factors are also relevant in the measurement's accuracy. The proportion of sample and enveloper volume (S/E) is an important factor to consider; when the S/E is low, the chamber volume occupied by the sample is low, then the difference between the displacement of the plunger position is small, resulting in inaccurate results. Otherwise, if the S/E is high, the sample particles will not be completely involved, promoting particle agglomeration, affecting the analysis accuracy [31]. The same concept is valid for choosing the chamber for the analysis that's consider the relation between the sample and enveloper volumes.

[2] Agglomerate - Consist of a consolidated assemblage of particles.

The conversion factor (K) is one of the parameters that directly affect the accuracy of the measurements [30,31]; this mathematical conversion is associated to the enveloper, and also to the shape and roughness of the sample's particles. The application of this automatized powder pycnometry using Geopyc instrument is limited by the particle size distribution of the commercial enveloper (Dryflo®); the manufacturer (Micromeritics) recommends the analysis of samples with particles size larger than 2 mm, because of that, many studies apply powder pycnometry only for pellets or coarse materials for envelope and bulk volume determinations.

Actually, PP could be properly applied for envelope volume of fragments in many areas, such as coarse recycled aggregates (particle size greater than 2 mm), petroleum drilling sidewall core fragments or control quality of tables for pharmaceutical area. The substitution of the enveloper by another material with similar characteristics, but smaller particle size would provide the extension in the application of this technique. The extension could potentially engage new applications such as for PP and porosity evaluation for well log drilling cuttings samples, soil and polymer microspheres for medical applications.

This work presents alternative envelopers to be applied for the assessment of envelope density of fine recycled aggregates. Another important contribution of this study is evaluating the porosity of FRA sands in fine and medium fractions by the association of powder and gas pycnometry.

2. Materials and methods

2.1. Materials

Three samples were used in this work: standard commercial natural river sand (RS) and two fine recycled aggregates (FRA) with low and high porosity, respectively. The processing for obtaining those FRA was previously detailed in literature [6] and consisted of jaw crushing (primary and secondary stages) and tertiary crushing by Vertical Shaft Impactor (VSI) crusher; in sequence, the attained product was then concentrated by magnetic separation for obtaining products with different porosities

The sands were hereby named MG and NM, representing the magnetic and non-magnetic product, respectively (Table 1.

The MG and NM materials were sieved into two fractions: medium (M) (0.300–1.180 mm) and fine (F) (0.074–0.300 mm) fractions and characterized by mercury intrusion porosimetry, dynamic image analysis, X-ray Microtomography, helium and powder pycnometry (PP) techniques.

Preliminary tests were performed to choose an ideal enveloper material; some common materials initially were tested, such as, baking powder, wheat flour, graphite (dry lubricant), talcum powder, grounded DryFlo® and glass microspheres (IM16K®).

Based on the required properties for the new enveloper obtained in the preliminary tests, new enveloper materials were selected such as carbon (Carb) and ceramic (Cerm) microspheres, that were also characterized by He pycnometry, dynamic image analysis, X-ray microtomography (Micro-CT) and PP techniques.

2.2. Characterization

2.2.1. Dynamic image analysis (DIA)

The particles size and shape distributions of the characterized samples (recycled sands and envelopers) were carried out by dynamic images analyses on the Retsch equipment, model Camsizer XT or L, according to the procedure described by the international standard ISO 13322-2/2006.

The DIA analyses converts the shadow projections of particles into binary images. The Camsizer XT was employed for enveloper DIA analysis. The equipment is indicated for particles size distributions between 1 μm to 3 mm. The preparation procedure for DIA analysis was the

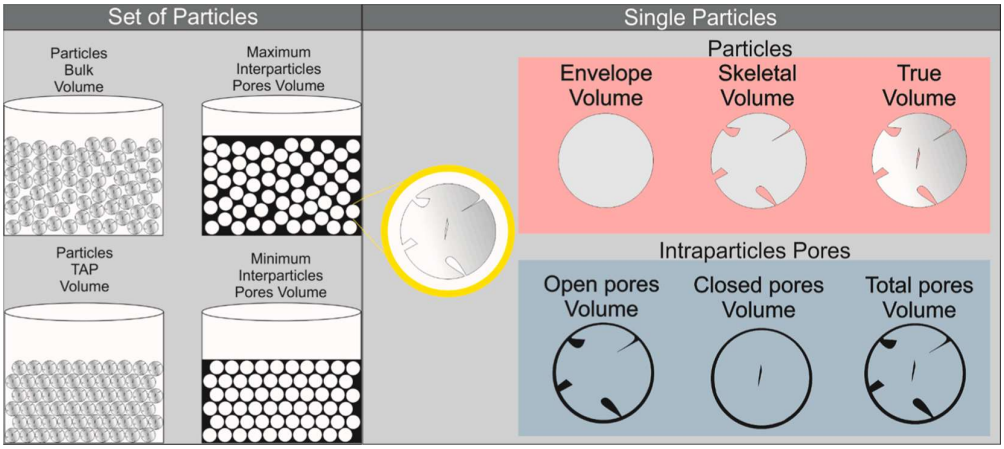

Fig. 1. Particles and pore volumes considering a set of particles and single particles.

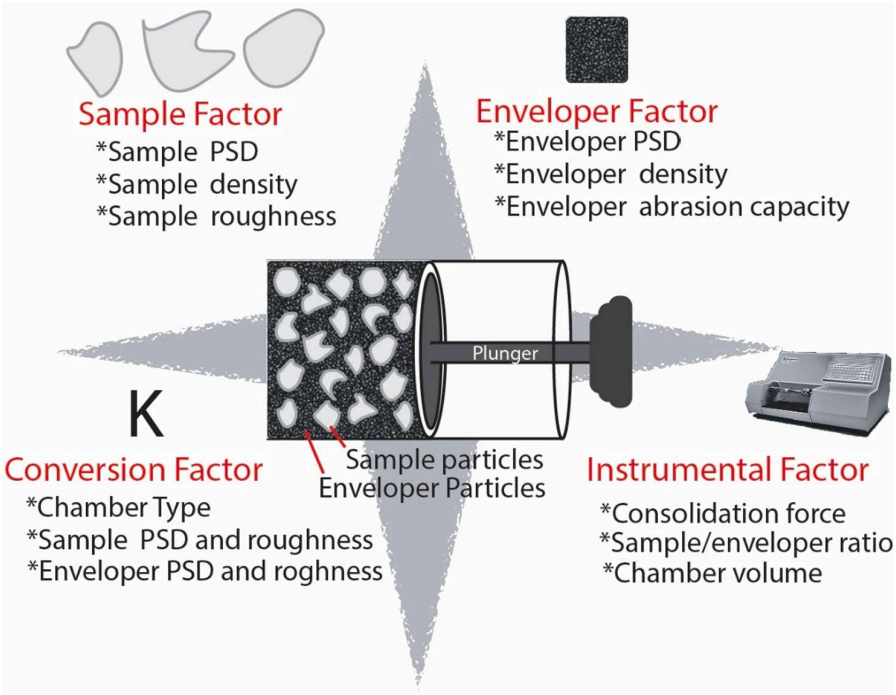

Fig. 2. The four main factors influencing the envelope volume determination by automated powder pycnometry.

Table 1
Sample's identification and nominal particles size interval.

Samples				
NS	MG_F	MG_M	NM_F	NM_M
Natural sand (0.60–1.18 mm)	Magnetic fraction Urbem Fine (0.074–0.30 mm)	Medium (0.300–1.180 mm)	Non-magnetic fraction Urbem Fine (0.074–0.30 mm)	Medium (0.300–1.180 mm)

dispersion in isopropanol, and sonication for 1 min (accessory "X-Flow").

The Camsizer L was used for sand analysis. The equipment is indicated for particles size distributions between 20 μm to 30 mm. No preparation is needed in this case, the sample fall in analysis chamber via a vibratory feed chute. The analysis considered more than 100,000 particles (natural sand (NS) - "178,000 particles"; MG_F "46,676,661 particles"; MG_M "1,312,226 particles"; NM_F "22,712,154 particles"; NM_M "11,828,931 particles).

2.2.2. *Mercury intrusion porosimetry (MIP)*

The MIP analysis were performed in accordance with ISO 15901–1/2016 (AutoPore IV equipment from Micromeritics); an appropriate bulb/rod assembly was used for the analysis. Experimental parameters were: Hg density (13.53 g/cm^3), Hg surface tension (0.485 N/m), contact angle 130° and equilibrium time of 20 s. The intruded volume of mercury was determined in stepwise mode with filling pressure of 0.00696 MPa (1 psi), the intrusion pressure was gradually increased until reach 414 MPa (60,000 psi). The volume of the sample intrusion mercury is a function of the applied hydrostatic pressure, which is related to the pore diameter by the Laplace equation (Eq. (1)) [38].

The mercury porosimetry tests were performed in duplicate to increase representativeness and reliability of the results, therefore, an average value was adopted between the two tests. Samples were homogenized and sampled to mitigate heterogeneity. The threshold pressure was selected sample by sample to calculate the porosity by MIP.

2.2.3. X-ray microtomography (Micro-CT)

The medium fraction of magnetic product was prepared trying to simulate PP analysis with sample/enveloper proportion (S/E) in volume (S/E equal to 1/3). The powder materials were disposed in a 1 mL syringe and homogenized with plunger until no more particles are observed on the syringe walls, after the plunger were pressed as to simulate the chamber compression and fixed applying silicone glue. The images were acquired in Zeiss Xradia Versa XRM-510 on the mode "core" and "zoom" (Table 2

2.2.4. Helium pycnometry (HeP)

The skeletal volume determination was performed by Helium gas pycnometry on Micromeritics model AccuPyc II 1340 equipment. Sands (recycled and natural) and enveloper samples were previously dried at 60 °C for 24 h, aiming to remove water molecules present on the surface and pores of the materials. After cooling in laboratory desiccator under reduced pressure, 70–80% of the chamber was filled with the materials for analysis. Five measurements were performed for each sample with 10 purge and 5 analysis cycles.

2.2.5. Powder pycnometry (PP)

Experimental analyses were performed at Geopyc equipment in a chamber with diameter of 50.8 mm, consolidation force of 145 N (ideal for this chamber size recommended by the equipment manual) and volumetric ratio of 1/3 sample and 2/3 enveloper. The K factor was initially obtained by analyzing a reference natural sand (NS) as standard material in triplicate.

Some preliminary tests were conducted to choose materials capable of substitute the Dryflo enveloper and identify the most relevant properties for these materials. The preliminary tests were performed replacing Dryflo by six different materials: baking powder, wheat flour, graphite, talcum powder, grounded DryFlo and glass microspheres (IM16K®).

The analysis cycle consisted of 5 initial consolidation cycles and 5 measurements cycles. After the preliminary tests and identification of ideal enveloper properties, new envelopers (carbon (*Carb*) (SIGRADUR®) and ceramic (*Cerm*) (3 M−W610) microspheres) were selected for substitute the commercial Dryflo enveloper.

3. Results and discussion

3.1. Enveloper characterization

The preliminary enveloper materials were evaluated based on the premise an ideal enveloper material must have top particles size silly larger than largest pore throat of the samples, in order to cover all the surface, without invade the pores. However, the enveloper particles cannot have similar particle size of the samples to decrease the interparticle envelope/sample voids to increase the measure precision. The ideal particle size distribution for a new enveloper must be as narrowest as possible for create a homogeneous interparticle voids.

The grounded DryFlo presented low values of d_{10} (Table 3 considering the pores size distribution of recycled sand samples further analyzed; the comminution process could be carried out in a closed circuit with a screen of the desired size (around 10 μm), but grinding and sieving in this size are not practical.

The graphite, wheat flour and talcum powder materials presented optimum values of d_{10}, but wide particle size distribution. The envelopers that presented optimum particle size parameters, both in the terms of particle size distribution and also in d_{10} values were the IM16K® and baking powder materials (Table 3). The materials chosen were tested and problems were found in the employment of these materials as envelopers.

The baking powder material exhibits a significant variation of particle size distribution between products lots, so it would be difficult to evaluate results considering the heterogeneity of this enveloper material. This issue is not observed for IM16K® material, because it is a commercial material applied in construction, painting and coating, with controlled production conditions. However, IM16K® enveloper material presents density of ($d = 0.4739 \pm 0.0006$ g/cm^3). The density issues were not considered essential in the first tests, but it promote the segregation of the particles during the envelope density determination by powder pycnometry analysis.

None of the material tested in the preliminary test were good enough to replace the commercial Dryflo®. Meanwhile, the preliminary tests were essential to select new materials with ideal properties. By the way, new enveloper materials, *Cerm* and *Carb*, where selected considering some parameter such as: particle size distribution, skeletal density, sphericity and aspect ratio (Table 4).

The *Cerm* and *Carb* have a similar particle size distribution (Fig. 3: *Cerm*; d_{10}-9.5 μm, d_{50}-13.9 μm and d_{90}-19.3 μm and *Carb* d_{10}- 6.8 μm, d_{50} – 12.2 and d_{90}- 19.6 μm). The *Carb* present smaller particles when compared to *Cerm*, both envelopers exhibit d_{10} values lower than 10 μm.

The *Cerm* and *Carb* envelopers present round/ellipsoid particles with high sphericity and aspect ratio average of 0.837; 0.801 and 0.775; 0.726, respectively (Fig. 4).

3.2. FRA particles characterization

The particles of the enveloper materials present greater values of sphericity and aspect ratio when compared with the FRA samples as expected. The particle size distribution curves (Fig. 5) presents in accordance with the sieving process. The skeletal densities (Table 5) present similar values when compared with the enveloper materials, mostly for *Cerm* microspheres.

The aspect ratio and sphericity results of the FRA samples indicate elongated particles with lower sphericity when compared with natural sand (NS). No changes in the sphericity and aspect ratio values were observed for the fractions studied, thus indicating that the particle shape originates from the recycled aggregate comminution process.

Table 2
X-ray micro-CT acquisition image parameters.

Instrumental Parameters	Core	Zoom
Total Scan Time	1h30m	2 h
Objective	0.4x	4x
Source Settings	80 kV / 7 W	80 kV/7 W
Pixel size (μm)	3.5	1
Number of Views	1000	1000
Time per View (sec)	4	5
Resol. Detector (pixels)	2048x2048	2048x2048
Field of view (FOV - μm)	7,000	2,200
Source Filter	None (air)	None (air)
Source distance (mm)	13	13
Detector distance (mm)	105	25

Table 3
Particles representative size of the enveloper materials.

Enveloper Materials	d_{10} (μm)	d_{50} (μm)	d_{90} (μm)
Talcum powder	6.6	22.2	59.4
Baking powder	9.4	14.5	21.9
Wheat flour	15.7	68.8	156.7
Graphite	13.5	45.3	116.3
Grounded DryFlo	2.5	11.2	34.4
Glass microspheres IM16K®	12.0	19.9	32.7

dx – particle diameter in which x% of the sample is under this size.

Table 4
Particles size distribution, shape parameters and density of Cerm and Carb.

Envelopers	d_{10} (μm)	d_{50} (μm)	d_{90} (μm)	Sphericity (SPHT)	Aspect ratio (b/l)	Skeletal density He (g/cm^3)
Cerm	9.5	13.9	19.3	0.837	0.775	2.5160
Carb	6.8	12.2	19.6	0.801	0.726	2.1955

d_x – particle diameter in which x% of the sample is under this size.

3.3. FRA MIP analysis

The samples analyzed present pores smaller than 1 μm as evidenced in the MIP analysis (Fig. 6). The porosity of the samples is calculated by Eq. (2), which relates the envelope mercury volume to total mercury volume for each MIP analysis of particulate material; for that, is imperative to select the threshold pressure by graphical analysis. The proper selection of filling pressure is crucial for MIP analysis, so that mercury fills the spaces between particles, without penetrating the intraparticles pores. The selective rule adopted in consonance with graphical analysis to properly select the threshold pressure is that the pore size distribution must not be greater than 2% of the top sample particle size (d_{90}), i.e. for medium (0.300–1.18 mm) and fine sands (0.074–0.300 mm) were considered pores smaller than 23.6 μm and 6.0 μm, respectively.

$$Porosity(\%) = 1 - \frac{\rho_{env}}{\rho_{ske}} \quad (2)$$

The products obtained in the magnetic separation have different porosities; the MIP analysis indicates that the magnetic fraction presents greater porosity in comparison to the non-magnetic fraction (Table 6. The threshold pressures and porosity for .MG_F, MG_M, NM_F and NM_M samples were 35 psi – 15.9%, 31 psi – 12.7%, 35 psi – 4.04% and 30 psi – 4.09% respectively.

The sieving process does not change the pore size distribution, only affects the porosity of the sample, i.e., porous phases are more concentrated at the magnetic product and increases on fine fraction (MG_F), as indicated by the literature [5]. Otherwise, the magnetic separation process affects the porosity and also the pores size distribution. The magnetic sample presents smaller pores when compared with non-magnetic in both fractions. The literature evidence MIP curves similar to the present study [39], especially for magnetic fraction. Pressure above 4,000 psi lead to the materials compression as reported in literature, after 12,000 Psi (10 nm) it become critics; this phenomena is observed in both MG samples with higher porosity and smaller pores [40].

The studies developed by Ulsen *et al* (2013) [6], indicate that magnetic products present a cement paste enrichment, and therefore an increase in porosity as indicated in accordance with the present study. The results indicate that the magnetic susceptibility is an important differentiating property between the residual cement paste and the non-porous mineral fraction [6]. The results highlight the importance of the efficient processing of the recycled aggregate in order to concentrate the minerals phase, which is corroborated by literature [9].

3.4. FRA powder pycnometry analysis

The evaluation of abrasion of FRA samples during the powder pycnometry analysis was carried out by weighing and sieving (0,074 mm for fine sand and 0,300 mm for medium sand) the samples before and after the analysis cycles and no changes in the mass were observed above 0.01%.

The optimum ratio of sample and enveloper volume is obtained experimentally during the preliminary, in the case of the sample studied only two conditions were tested: 33% of sample (1/3) with 66% of enveloper (2/3) and 50 % of sample (1/2) with 50% of enveloper (1/2). The lower standard deviation between measurements was obtained for the first condition (1/3 sample and 2/3 of enveloper).

The calibration of the equipment requires a standard material with defined or no porosity with similar characteristics to the analyzed samples for estimating the "K" factor; in this work, natural sand (NS) was used as standard material. The values of the correction factor (K) obtained after the calibration demonstrate differences between the envelopers materials (Table 7.

Therefore, the results in Table 7 indicate that the replacement of the enveloper material results in alteration of the correction factor (Dryflo® correction factor for 50.8 mm chamber, K = 2.0373 cm^3/mm) mainly for

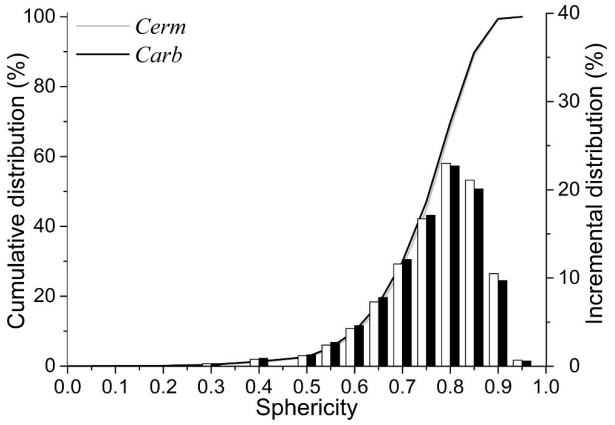

Fig. 4. Enveloper sphericity (SPHT) parameter Cerm (light gray) and Carb (black).

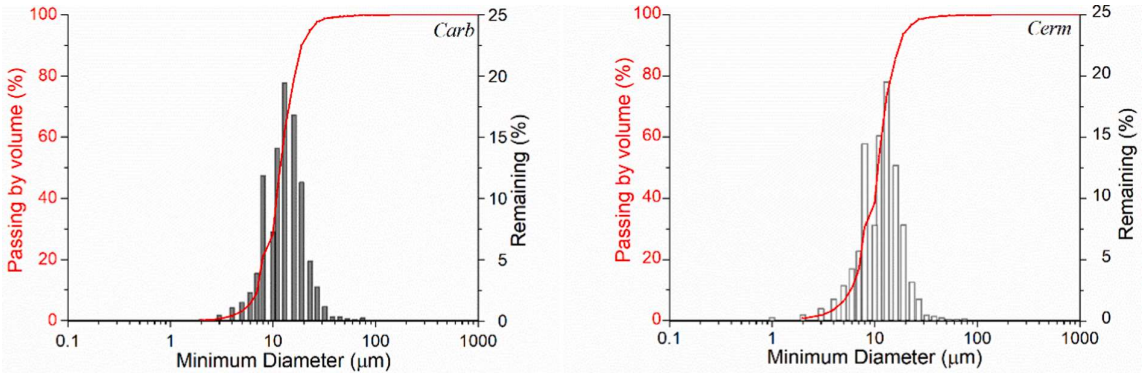

Fig. 3. Particles size distribution of envelopers materials.

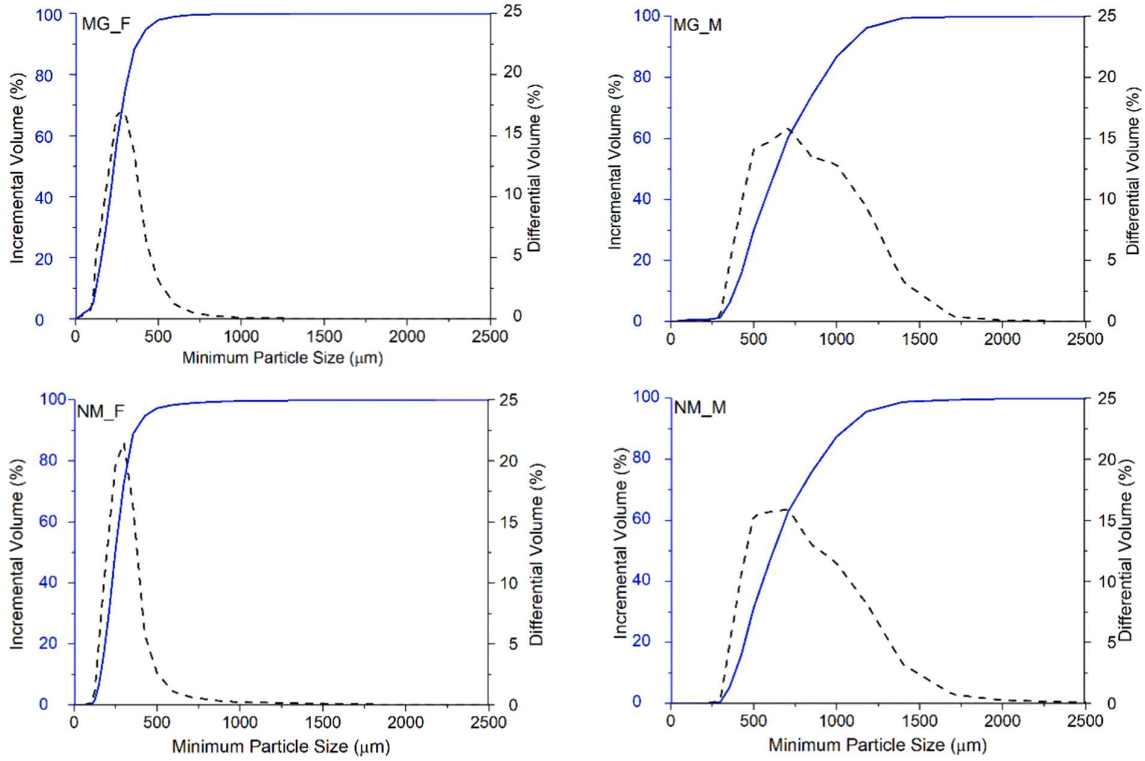

Fig. 5. Recycled sands particle size distribution (DIA).

Table 5
Particles size distribution, shape parameters and density of recycled sands.

Samples	d_{10} (μm)	d_{50} (μm)	d_{90} (μm)	SPHT	Aspect Ratio (b/l)	Skeletal Density (He_Pyc) (g cm^{-3})
NM_F	192	298	435	0.740	0.635	2.6161 ± 0.0008
NM_M	393	620	1,063	0.749	0.694	2.6392 ± 0.0004
MG_F	125	227	354	0.711	0.662	2.5182 ± 0.0014
MG_M	457	755	1,237	0.740	0.653	2.5753 ± 0.0012
NS	668	882	1,159	0.804	0.715	2.5690 ± 0.0006

d_x – particle diameter in which x% of the sample is under this size.

Carb enveloper. That indicates the applied enveloper material have a significant contribution for the correction factor.

During the powder pycnometry (PP) measurements with the *Carb,* its observed large amount of enveloper volume evades the chamber (Fig. 7). The fact is related to the high lubricating capacity of the graphite present in carbon microspheres. Graphite is a lubricant material formed by layers of sp^2-hybridized carbon atoms, where each layer is stacked together by weak van der Waals forces. Its layered structure and the intermolecular forces between the layers that give this material its lubricating properties [41].

The lubricant property of *Carb* initially was considered positive, since it should facilitate the accommodation of the enveloper in between the particles of the solid samples increasing the packing ability of the enveloper, but the high-volume evading from the chamber during the measurements may compromise its application as enveloper material.

The PP measurements (Table 8) show small standard deviation in envelope density determination for medium sand FRA, which may be related to the large difference in particle size between the enveloper and samples.

The fine sand fraction PP analysis indicates different results when comparing the tested envelopers. The results inaccuracy is not only related to enveloper evade effect in case of *Carb*, but it is probably due to the difference between the maximum particle size of the enveloper materials *Cerm* (d_{90} around 19 μm, Table 4 and the minimum particle size (MG_F (d_{10} = 125 μm) and NM_F (d_{10} = 192 μm, Table 5 of the fine fraction of FRA samples. Therefore, the results pointed out that a smaller enveloper size must be used in fractions finer than 0.30 mm.

The *Cerm*, for example, present particle size, d_{90},10–15% in size compared to inferior particle size, d_{10}, of fine sand, for medium sand particle this size represents 3–5% in size. This phenomenon considerably increases the number of voids between the sample and envelope particles.

Another important consideration is related to the natural sand used for the K_{factor} determination, that presents particle size distribution similar to the medium FRA fraction. Probably the conformance of the material behavior is different in distinct fractions, further studies employing fine natural sand in K_{factor} determination could be performed in order to improve the results of FRA fine fraction.

The experimental parameter of consolidation force was not approached in this work for PP analysis, the value recommended by the manufacturer's manual was used for the analysis chamber. The consolidation force is the parameter that affects the degree of packaging, which is the ability of the enveloper particles surround the sample particles in order to minimize the voids between the particles and also affects the samples abrasion during the analysis.

3.5. Porosities: Pycnometry association vs MIP analysis

The porosity of the recycled sands (Fig. 8) suggests that the method for the determination of open pores by the association of pycnometry techniques is comparable to the MIP (Table 9), especially in the analysis for medium fractions (0.300–1.180 mm) with *Cerm* material as enveloper.

The porosity in fine fraction (0.074–0.300 mm) for MIP and pycnometry association techniques were not comparable, even so, the

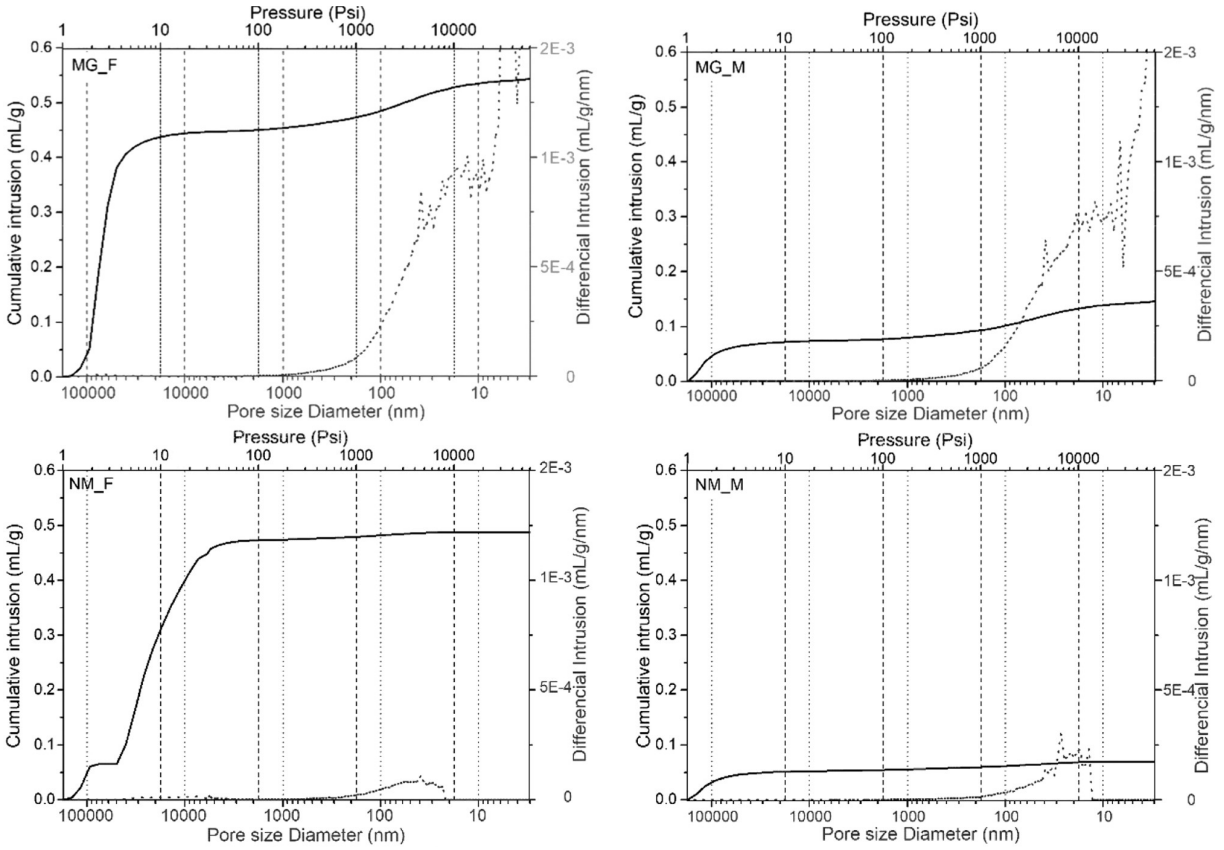

Fig. 6. Recycled sands cumulative mercury intrusion and differential mercury intrusion curves.

Table 6
Porosity and median pore size by volume, MIP parameters.

Sample	Porosity (%) (MIP)	Median pore diameter (nm)
MG_F	15.9 ± 0.3	11.48
MG_M	12.7 ± 0.9	10.30
NM_F	4.04 ± 0.1	44.50
NM_M	4.09 ± 0.8	25.97

Table 7
Correction factor (K) for envelopers materials *Carb* and *Cerm*.

Standard Sample	K (cm^3/mm) *Carb*	K (cm^3/mm) *Cerm*
Natural sand 1	2.0361	1.8489
Natural sand 2	2.0231	1.8734
Natural sand 3	2.0362	1.8750
Mean	2.0318	1.8658
Std Desv	0.0075	0.0146

Fig. 7. Powder pycnometry analysis employing the envelopers.

porosity of the NM_F sample present better results when compared with MG_F samples. It is important to consider that the magnetic fraction present higher porosity, and consequently high cement paste content. The cement paste impacts the roughness of the material and possibly impacting negatively the PP measurements. The conformance of the enveloper surrounding the samples affects directly the PP measurement.

The small particle size differences between the enveloper and samples increase the voids volumes between the particles. Thus, it increases the PP measurement inaccuracy. In order to compare the MIP and pycnometry association for fine fraction, a new enveloper must be applied with small particle size than the enveloper tested. Another way to improve the results of fine fraction is evaluate the K_{factor} considering an restrict particle size distribution similar with the analyzed samples.

The equipment's manual recommends for envelope density determination by Geopyc, samples with particle size greater than 2 mm. Considering this recommendation, the particle size distribution of Dryflo® was performed (d_{90} = 227 μm). That's indicates the sample particles (d_{10}) are 10 times greater than enveloper material particles.

Table 8
Envelope density of recycled sands employing *Carb* and *Cerm* as enveloper materials.

Samples	*Cerm*	*Carb*
Envelope Density	(g/cm^3)	(g/cm^3)
MG_M	2.1432 ± 0.0210	2.2258 ± 0.0345
MG_F	1.9327 ± 0.0292	1.8699 ± 0.0129
NM_M	2.5395 ± 0.0145	2.5475 ± 0.0239
NM_F	2.4728 ± 0.0173	2.3543 ± 0.0069

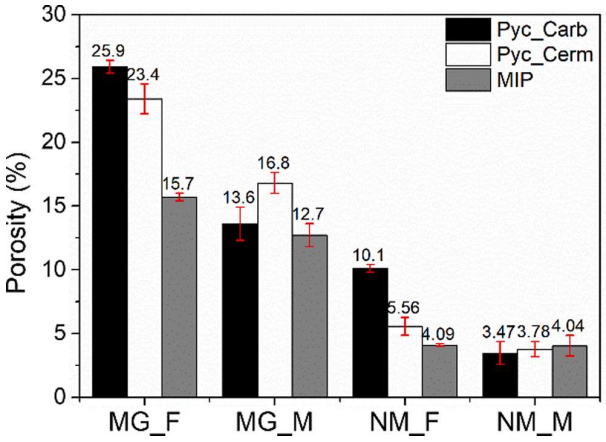

Fig. 8. Porosity of FRA by MIP (gray) and pycnometry association employing the envelopers.

Table 9
Determination of the recycled aggregates porosity by MIP and association of gas and powder pycnometry techniques.

Porosity (%) Samples	Pyc_*Carb*	Pyc_*Cerm*	MIP
MG_F	25.9 ± 0.5	23.4 ± 1.2	15.9 ± 0.3
MG_M	13.6 ± 1.3	16.8 ± 0.8	12.7 ± 0.9
NM_F	10.1 ± 0.3	5.56 ± 0.7	4.04 ± 0.1
NM_M	3.47 ± 0.9	3.78 ± 0.6	4.09 ± 0.8

Considering the smallest particle size values of the samples (d_{10}) and top size of the tested envelopers (d_{90}), the analyzed FRA samples show sample/enveloper size relation in percentage of: MG_F (9.95%), MG_M (20.4%), NM_F (6.48%), NM_M (23.7%) for *Cerm* and MG_F (9.80%), MG_M (20.1%), NM_F (6.38%), NM_M (23.3%) for *Carb*.

3.6. X-ray microtomography (Micro-CT)

The tomography characterization was performed in order to evidence the packing ability of that is considered the best enveloper material for PP analysis. The images show high roughness on the particles surface, as well as distinct particles shape and minerals association in the sand, i.e., the presence of high-density mineral grains (lighter grey levels of the image, Fig. 9).

The 2D images of X-ray micro-CT longitudinal slice (Fig. 10) represent the enveloper particle packing, by means of its interparticle porosity (segmented in blue) surrounding the MG_M particles. The acquisition of images by Micro-CT in packed particles systems with different dimensions, requires making selections.

In the first section, image acquisition is performed in all material increasing the representability, but decreasing the image resolution, which impacts negatively in the segmentation of enveloper particles and pore space. In the second section, image acquisition was performed in high resolution, however limiting the size of the analyzed volume, thus compromising representability.

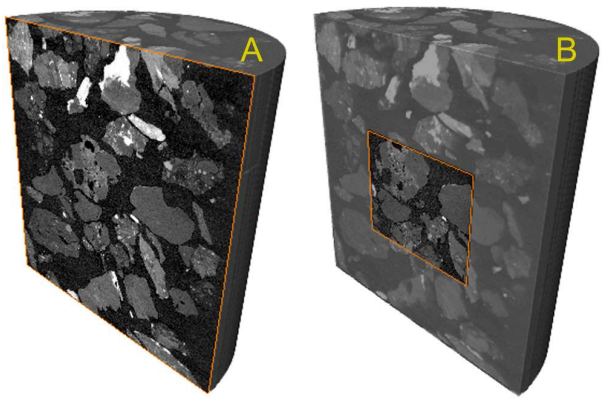

Fig. 9. X-ray Micro-CT core image of syringe filled with MG involved in Cerm particles (A) core image (voxel size, 3.5 μm) and (B) zoom image (voxel size, 1 μm).

Another phenomenon that's requires attention, and evidence and extremely important concept for envelope density measurements are related to the "shadow zones" (red circles in Fig. 10). The shadow zones are defined as the region in which the enveloper particles were not able to access, given a limit of enveloper particle size or flow rate. The Micro-CT experiments were conducted to simulate the conditions of automatized power pycnometry, but without employ vibrations in sample preparation. The vibration contributes to the packing ability of envelopers, so improvement in the sample preparation and image acquisition is required for a correct porosity determination by micro-CT.

The particle size distribution and particles flow rate of enveloper material impact the samples envelope volume measurement. These parameters are critical to evaluate the envelope effectiveness in determining envelope density in samples with high roughness. Thus, employing different envelopers materials for samples envelope density characterization, the results will not be the same, but similar.

The Micro-CT characterization indicates a good packaging of the *Cerm* particles surrounding recycled sand particles (MG_M) that is corroborated by the porosity measurements, despise of "shadow zones".

4. Conclusion

The replacement of the commercial DryFlo® by microsphere of ceramic (*Cerm*) and carbon (*Carb*) as envelopers contribute to extending the application of PP technique to samples with particles larger than 0.3 mm. The associated method of helium gas and powder pycnometry present simple and quick results (20 min) comparable to MIP for recycled sand in medium fraction (0.300–1.180 mm), with good accuracy for porosity determination.

The tested envelopers (*Cerm* and *Carb*) replaced properly the commercial enveloper for the envelope density measurements for FRA samples at a medium fraction (0.300–1.180 mm). The best-tested enveloper material applied for FRA samples were *Cerm*, factor such as similar sample density, narrow particle size distribution, flow rate and spherical shape are determinant for improve the conformance.

The envelope retention in the analysis chamber also contributes to the measurement accuracy, thus the employment of *Carb* as an enveloper presents significant deviations in porosity analysis. The aspects such as K_{factor} and the relation between enveloper and sample PSD is an important topic for the accuracy of the envelope density determination by PP, mainly for fine fraction analysis (0.074–0.300 mm).

CRediT authorship contribution statement

Rafael dos Santos Macedo: Conceptualization, Methodology,

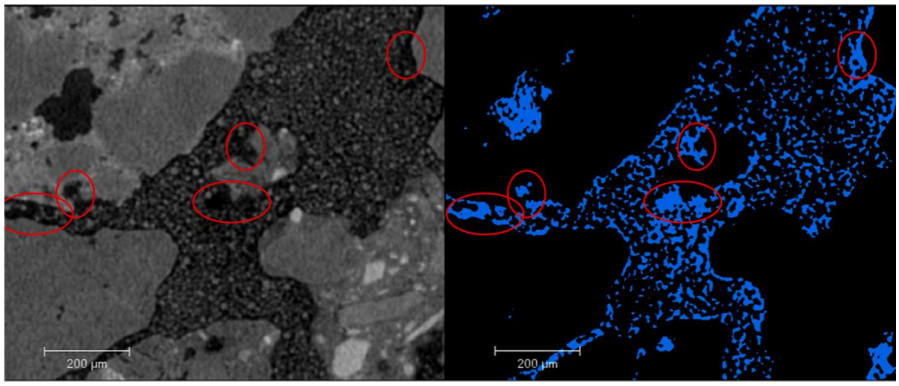

Fig. 10. X-ray Micro-CT slice image (A) envelopers and samples particles (B) interparticles voids.

Investigation, Formal analysis, Writing – original draft,**Carina Ulsen:** Funding acquisition, Conceptualization, Supervision, Resources, Writing – review & editing,**Ana Y. Jacomo:**Methodology, Investigation, Formal analysis,**Paula O. Figueiredo:**Investigation, Formal analysis, **Guilherme P. Nery:**Writing – review & editing, Resources,**Daniel Uliana:**Investigation, Formal analysis,**Anette Müller:**Resources, Writing – review & editing, Funding acquisition.

Declaration of Competing Interest

The authors declare that they have no known competing financial interests or personal relationships that could have appeared to influence the work reported in this paper.

Acknowledgments

The authors gratefully acknowledge FAPESP (the State of São Paulo Research Foundation) for the financial support through process 2010-15543-1, CNPq-CAPES process 88881 068109 2014-01 and Technological Characterization Laboratory (LCT). The information and views set out in this study are those of the authors and not necessarily reflect the opinion of the founding agencies.

References

[1] M.H.Z. Faruqi, F.Z. Siddiqui, A mini review of construction and demolition waste management in India, Waste Manag. Res. 38 (7) (2020) 708–716, https://doi.org/10.1177/0734242X20916828.
[2] P. Sormunen, T. Kärki, Recycled construction and demolition waste as a possible source of materials for composite manufacturing, J. Build. Eng. 24 (2019), 100742, https://doi.org/10.1016/j.jobe.2019.100742.
[3] A.E.B. Cabral, V. Schalch, D.C.C.D. Molin, J.L.D. Ribeiro, Performance estimation for concretes made with recycled aggregates of construction and demolition waste of some Brazilian cities, Mater. Res. 15 (2012) 1037–1046, https://doi.org/10.1590/S1516-14392012005000119.
[4] R. Islam, T.H. Nazifa, A. Yuniarto, A.S.M. Shanawaz Uddin, S. Salmiati, S. Shahid, An empirical study of construction and demolition waste generation and implication of recycling, Waste Manag. 95 (2019) 10–21, https://doi.org/10.1016/j.wasman.2019.05.049.
[5] C.M. Mah, T. Fujiwara, C.S. Ho, Construction and demolition waste generation rates for high-rise buildings in Malaysia, Waste Manag. Res. 34 (12) (2016) 1224–1230, https://doi.org/10.1177/0734242X16666944.
[6] C. Ulsen, H. Kahn, G. Hawlitschek, E.A. Masini, S.C. Angulo, Separability studies of construction and demolition waste recycled sand, Waste Manag. 33 (3) (2013) 656–662, https://doi.org/10.1016/j.wasman.2012.06.018.
[7] C. Ulsen, H. Kahn, G. Hawlitschek, E.A. Masini, S.C. Angulo, V.M. John, Production of recycled sand from construction and demolition waste, Constr. Build. Mater. 40 (2013) 1168–1173, https://doi.org/10.1016/j.conbuildmat.2012.02.004.
[8] S. Delvoie, Z. Zhao, F. Michel, L. Courard, Market analysis of recycled sands and aggregates in NorthWest Europe: Drivers and barriers, in: IOP Conf. Ser. Earth Environ. Sci., 2019: pp. 1–8. 10.1088/1755-1315/225/1/012055.
[9] C. Ulsen, E. Tseng, S.C. Angulo, M. Landmann, R. Contessotto, J.T. Balbo, H. Kahn, Concrete aggregates properties crushed by jaw and impact secondary crushing, J. Mater. Res. Technol. 8 (1) (2019) 494–502, https://doi.org/10.1016/j.jmrt.2018.04.008.
[10] P. Gonçalves, J.D. Brito, Recycled aggregate concrete (RAC) – comparative analysis of existing specifications, Mag. Concr. Res. 62 (2010) 339–346, https://doi.org/10.1680/macr.2008.62.5.339.
[11] M.B. Leite, V.M. Santana, Evaluation of an experimental mix proportion study and production of concrete using fine recycled aggregate, J. Build. Eng. 21 (2019) 243–253, https://doi.org/10.1016/j.jobe.2018.10.016.
[12] M. Quattrone, B. Cazacliu, S.C. Angulo, E. Hamard, A. Cothenet, Measuring the water absorption of recycled aggregates, what is the best practice for concrete production? Constr. Build. Mater. 123 (2016) 690–703, https://doi.org/10.1016/j.conbuildmat.2016.07.019.
[13] C.S. Poon, Z.H. Shui, L. Lam, Effect of microstructure of ITZ on compressive strength of concrete prepared with recycled aggregates, Constr. Build. Mater. 18 (6) (2004) 461–468, https://doi.org/10.1016/j.conbuildmat.2004.03.005.
[14] H. Maimouni, S. Remond, F. Huchet, P. Richard, V. Thiery, Y. Descantes, Quantitative assessment of the saturation degree of model fine recycled concrete aggregates immersed in a filler or cement paste, Constr. Build. Mater. 175 (2018) 496–507, https://doi.org/10.1016/j.conbuildmat.2018.04.211.
[15] ABNT, Fine aggregate - Test method for water absorption, NBR NM30. (2001).
[16] ASTM C128-15, Standard Test Method for Density, Relative Density (Specific Gravity), and Absorption, Am. Soc. Test. Mater. (2015) 1–6.
[17] M.E. Sosa, L.E. Carrizo, C.J. Zega, Y.A. Villagrán Zaccardi, Water absorption of fine recycled aggregates: effective determination by a method based on electrical conductivity, Mater. Struct. 51 (2018) 127, https://doi.org/10.1617/s11527-018-1248-2.
[18] J. Naël-Redolfi, E. Keita, N. Roussel, Water absorption measurement of fine porous aggregates using an evaporative method: Experimental results and physical analysis, Cem. Concr. Res. 104 (2018) 61–67, https://doi.org/10.1016/j.cemconres.2017.11.003.
[19] S. Diamond, Mercury porosimetry, Cem. Concr. Res. 30 (10) (2000) 1517–1525, https://doi.org/10.1016/S0008-8846(00)00370-7.
[20] R.A. Cook, K.C. Hover, Mercury porosimetry of hardened cement pastes, Cem. Concr. Res. 29 (6) (1999) 933–943, https://doi.org/10.1016/S0008-8846(99)00083-6.
[21] Y.C. Choi, J. Kim, S. Choi, Mercury intrusion porosimetry characterization of micropore structures of high-strength cement pastes incorporating high volume ground granulated blast-furnace slag, Constr. Build. Mater. 137 (2017) 96–103, https://doi.org/10.1016/j.conbuildmat.2017.01.076.
[22] Y. Gao, K. Wu, J. Jiang, Examination and modeling of fractality for pore-solid structure in cement paste: Starting from the mercury intrusion porosimetry test, Constr. Build. Mater. 124 (2016) 237–243, https://doi.org/10.1016/j.conbuildmat.2016.07.107.
[23] . Giesche, Mercury Porosimetry, in: F. Schuth, S. Kenneth, W. Sing, J. Weitkarnp (Eds.), Handb. Porous Solids, 1st ed., WILEY-VCH, Weinheim, 2002: pp. 309–349.
[24] H. Giesche, Mercury porosimetry: A general (practical) overview, Part. Part. Syst. Charact. 23 (1) (2006) 9–19, https://doi.org/10.1002/ppsc.v23:110.1002/ppsc.200601009.
[25] ASTM C566-97(2004), Standard Test Method for Total Evaporable Moisture Content of Aggregate by Drying, ASTM Int. (2004) 1–3. 10.1520/C0566-97R04.2.
[26] P. Gentilini, O. Yazoghli-Marzouk, V. Delmotte, Y. Descantes, Determination of the water content of fillerised fine aggregates in the saturated surface dry state, Constr. Build. Mater. 98 (2015) 662–670, https://doi.org/10.1016/j.conbuildmat.2015.08.131.
[27] P.A. Webb, Volume and Density Determinations for Particle Technologists, Micromeritics Instrum. Corp. (2001) 1–16. http://www.micromeritics.com/Repository/Files/density_determinations.pdf.
[28] A. Abbas, G. Fathifazl, B. Fournier, O.B. Isgor, R. Zavadil, A.G. Razaqpur, S. Foo, Quantification of the residual mortar content in recycled concrete aggregates by image analysis, Mater. Charact. 60 (7) (2009) 716–728, https://doi.org/10.1016/j.matchar.2009.01.010.
[29] S.P.E. Forsmo, J.P. Vuori, The determination of porosity in iron ore green pellets by packing in silica sand, Powder Technol. 159 (2) (2005) 71–77, https://doi.org/10.1016/j.powtec.2005.05.032.

[30] J.B. Wade, G.P. Martin, D.F. Long, An assessment of powder pycnometry as a means of determining granule porosity, Pharm. Dev. Technol. 20 (3) (2015) 257–265, https://doi.org/10.3109/10837450.2013.860550.
[31] C.E. Brewer, V.J. Chuang, C.A. Masiello, H. Gonnermann, X. Gao, B. Dugan, L. E. Driver, P. Panzacchi, K. Zygourakis, C.A. Davies, New approaches to measuring biochar density and porosity, Biomass Bioenergy. 66 (2014) 176–185, https://doi.org/10.1016/j.biombioe.2014.03.059.
[32] F. Rabier, M. Temmerman, T. Bohm, H. Hartmann, P. Daugbjerg Jensen, J. Rathbauer, J. Carrasco, M. Fernandez, Particle density determination of pellets and briquettes, Biomass and Bioenergy. 30 (11) (2006) 954–963, https://doi.org/10.1016/j.biombioe.2006.06.006.
[33] T. Tracz, Open porosity of cement pastes and their gas permeability, Bull. Polish Acad. Sci. Tech. Sci. 64 (2016) 775–783, https://doi.org/10.1515/bpasts-2016-0086.
[34] R. Ramachandran, J.M.H. Poon, C.F.W. Sanders, T. Glaser, C.D. Immanuel, F. J. Doyle, J.D. Litster, F. Stepanek, F.Y. Wang, I.T. Cameron, Experimental studies on distributions of granule size, binder content and porosity in batch drum granulation: Inferences on process modelling requirements and process sensitivities, Powder Technol. 188 (2008) 89–101, https://doi.org/10.1016/j.powtec.2008.04.013.
[35] F. Cannova, M. Davidson, L. Forte, B. Sadler, Influence of Crushing Technology and Particle Shape on the Bulk Density of Anode Grade Petroleum Coke, in, Light Met. (2018) 1169–1177, https://doi.org/10.1007/978-3-319-72284-9_153.
[36] T. Zdeb, Effect of vacuum mixing and curing conditions on mechanical properties and porosity of reactive powder concretes, Constr. Build. Mater. 209 (2019) 326–339, https://doi.org/10.1016/j.conbuildmat.2019.03.116.
[37] J. Rouquerol, D. Avnir, C.W. Fairbridge, D.H. Everett, J.M. Haynes, N. Pernicone, J. D.F. Ramsay, K.S.W. Sing, K.K. Unger, Recommendations for the characterization of porous solids (Technical Report), Pure Appl. Chem. 66 (1994) 1739–1758, https://doi.org/10.1351/pac199466081739.
[38] L.M. Anovitz, D.R. Cole, Characterization and Analysis of Porosity and Pore Structures, Rev. Mineral. Geochemistry. 80 (1) (2015) 61–164, https://doi.org/10.2138/rmg.2015.80.04.
[39] S. Cheng, Z. Shui, T. Sun, R. Yu, G. Zhang, Durability and microstructure of coral sand concrete incorporating supplementary cementitious materials, Constr. Build. Mater. 171 (2018) 44–53, https://doi.org/10.1016/j.conbuildmat.2018.03.082.
[40] R.A. Cook, K.C. Hover, Mercury porosimetry of cement-based materials and associated correction factors, Constr. Build. Mater. 7 (4) (1993) 231–240, https://doi.org/10.1016/0950-0618(93)90007-Y.
[41] E.HL. Falcao, F. Wudl, Carbon allotropes: beyond graphite and diamond, J. Chem. Technol. Biotechnol. 82 (6) (2007) 524–531, https://doi.org/10.1002/(ISSN)1097-466010.1002/jctb.v82:610.1002/jctb.1693.